RHIC/AP/84

COMPARISON OF MEASURED AND COMPUTED DYNAMIC APERTURE FOR THE SPS AND THE HERA PROTON RING

O. BRÜNING[1], W. FISCHER[2], F. SCHMIDT[1] and F. WILLEKE[2]

[1] *CERN, CH–1211 Geneva 23, Switzerland*
[2] *DESY, Notkestraße 85, D–22603 Hamburg, Germany*

Submitted to the proceedings of the LHC Single Particle Dynamics Workshop, Montreux, 1996.

Nonlinear magnetic fields in conjunction with tune modulation can lead to chaotic particle motion and thereby limit the dynamic aperture of hadron storage rings. This is of particular interest for the LHC at injection energy where the field errors of the superconducting magnets and the beam size have their maximum.
The SPS dynamic aperture experiment was performed to study a controlled nonlinear machine under the influence of tune modulation. In parallel, long–term tracking simulations were done to test to which extend computer programs can predict the dynamic aperture under those conditions.
In a complementary experiment at the HERA proton ring the dynamic aperture was measured at injection energy under normal operating conditions. The computer simulations for these measurements included a very detailed model of the nonlinear magnetic fields which were measured for each individual magnet.

KEY WORDS: dynamic aperture, measurements, simulations

1 INTRODUCTION

Superconducting magnets, used in high energy storage rings, introduce unavoidably nonlinear field errors. Persistent currents lead to large systematic multipole errors while mechanical imperfections mainly cause randomly distributed nonlinearities. Moreover, the slow decay of the persistent currents is a source of additional random field errors since the decay rate may vary considerably from magnet to magnet. These nonlinear magnetic field errors and tune modulation, which arises for example from power supply ripple, can limit the single particle stability and thus the dynamic aperture.

Since there are no reliable analytical tools available for the computation of the dynamic aperture one has to rely on computer simulations. Element–by–element tracking programs like SIXTRACK[1] aim at simulating the particle motion in storage rings as realistically as possible and can be used to determine the border of stable motion. In dedicated experiments at the CERN SPS and the HERA proton ring the dynamic aperture was measured and the results are compared with such computer simulations. While a controlled nonlinear machine was studied in the

TABLE 1: Beam parameters for the dynamic aperture experiments at the SPS and the HERA proton ring.

	SPS	HERA–p
RF	off	on
Energy E [GeV]	120	40
1σ norm. emittance ϵ_n [mm mrad]	≈ 5 hor. and ver.	≈ 5 hor. and ver.
Momentum spread $\Delta p/p$	$\approx 10^{-3}$	$\approx 5 \cdot 10^{-4}$
Intensity I (beam current)	$< 10^{12}$ p (7 mA)	$\approx 2 \cdot 10^{12}$ p (13 mA) in 60 bunches $\approx 4 \cdot 10^{11}$ p (3 mA) in 10 bunches
Closed orbit rms	≤ 0.3 mm hor. and ver.	≤ 2 mm hor. and ver.
Linear coupling	$\mid Q_x - Q_z \mid \leq 0.003$	$\mid Q_x - Q_z \mid \leq 0.003$
Chromaticity $Q' = \Delta Q/(\Delta p/p)$	≈ 1 hor. and ver.	≈ 1 hor. and ver.
Total natural tune ripple depth	$1.1 \cdot 10^{-4}$	$4 \cdot 10^{-4}$

SPS experiments, the dynamic aperture of a superconducting machine was measured under normal operating conditions at the HERA proton ring.

The definition of the dynamic aperture in a real machine is somewhat ambiguous. In the experiments the aperture is filled by kicking the beam until a sizable particle loss can be observed. Therefore, we define the dynamic aperture as the maximum stable amplitude above which no particles survive a time interval of interest. We consider several minutes, a time usually needed for injection, when nonlinearities and the beam size have their maximum. The comparison of measured and computed amplitude dependent tunes serves as a first test of the storage ring models used in the simulations since this a characteristic property of any nonlinear machine.

2 THE EXPERIMENT AT THE SPS

Measurements were made with the set–up given in Tab. 1. Strong non–linearities were introduced by 8 powerful sextupoles. The natural tune ripple spectrum contained 7 major lines that add up to an amplitude of $0.5 \cdot 10^{-4}$, which is half of the total measured natural tune ripple depth. The working points (26.637, 26.533) and (26.605, 26.538) referred to as WP1 and WP2 respectively (see Fig. 1 (a)) were examined. In some cases additional tune modulation was introduced by a single quadrupole with a frequency of 9 Hz and an amplitude of $\Delta Q_x = 1.87 \cdot 10^{-3}$ and $\Delta Q_x = 0.55 \cdot 10^{-3}$ at WP1 and WP2 respectively. The ratio of horizontal and vertical ripple depth was $\Delta Q_x/\Delta Q_z = 1.75$.

2.1 Detuning and Instrumentation

With kicks of varying strength the detuning was measured as a function of the horizontal betatron amplitude. The tunes were computed from up to 8192 turns after the kick by FFT and phase advance averaging[2] leading to a precision of $5 \cdot 10^{-4}$. Fig. 1 (b) shows the comparison of the measured and calculated detuning at WP1. The agreement is good up to large amplitudes and the dependence of the detuning

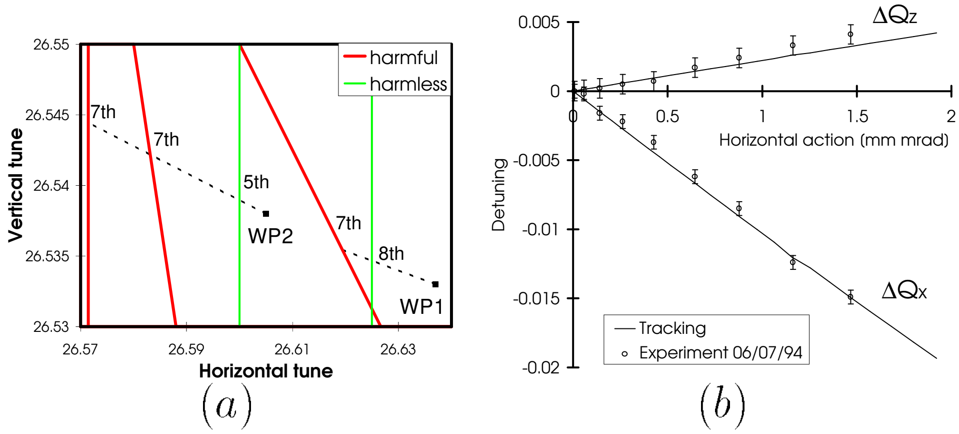

FIGURE 1: (a) The working points WP1 and WP2 in the tune diagram. Sum resonances up to order 8 are shown. The dotted lines show the detuning when the horizontal dynamic aperture is approached. (b) SPS detuning at working point WP1 with the set–up given in Tab 1.

on action ($\frac{x_{max}^2}{2\times\beta_x}$ at locations with $\alpha = 0$) is predominantly linear as expected from second order perturbation theory.

The kicked beam was observed by a flying carbon wire of 8 μm diameter and $0.4\,\mathrm{m}\cdot\mathrm{s}^{-1}$ speed. The position of the wire could be measured via an opto–electronic ruler with a resolution of 16 μm. The intensity of the kicked beam was reduced by $0.7 \cdot 10^{-4}$ per scan but no beam blow–up could be observed. The kicked beam produced a typical double peak structure in the wire scan profile (Fig. 2). The kick strength calculated from the distance between the peaks (see Fischer[4]) agreed within 10% with the kicker calibration. These beam profiles were also compared with scans from flying wires at different locations. The agreement amounted to some 5–10% which also increased the confidence in the knowledge of the β–functions around the ring.

2.2 Dynamic Aperture Measurements

Experimentally, the dynamic aperture was determined from the maximum base width of the wire scan profiles (Fig. 2). At the edge of the profile $5 \cdot 10^7$ protons (typically 10^{-4} of the intensity) can be clearly detected. In most cases 15 scans have been taken at time intervals of about 1 min.

In Fig. 3 four dynamic aperture measurements at WP1 with additional tune modulation are depicted. These curves were smoothed and the estimated error bars are shown in case #91 (a complete listing of all experimental runs can be found in Fischer[4]). The reproducibility of the experimental result was found to be within 2% for two measurements under the same conditions but 5 months apart (#62 and #76). Due to the rather large beam size the results depend on the measurement procedure: cases #62 and #76 were scraped horizontally after kicking, whereas

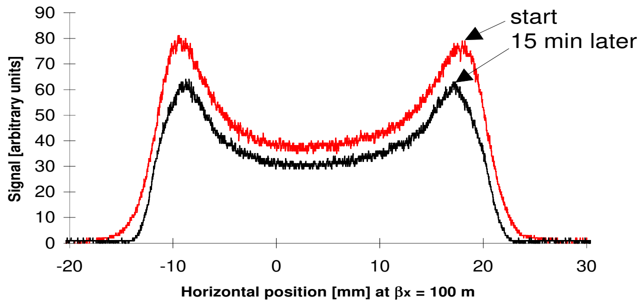

FIGURE 2: Evolution of the wire scan profile at WP1, tune ripple of 9Hz and $\Delta Q_x = 1.87 \cdot 10^{-3}$ (#78, no horizontal scraping).

cases #78 and #91 were left unscraped and in addition the latter case has been kept for some extra 15 min without additional tune modulation. Although these cases strongly differ initially, after 345 s the differences reduce to about 5% in the dynamic aperture.

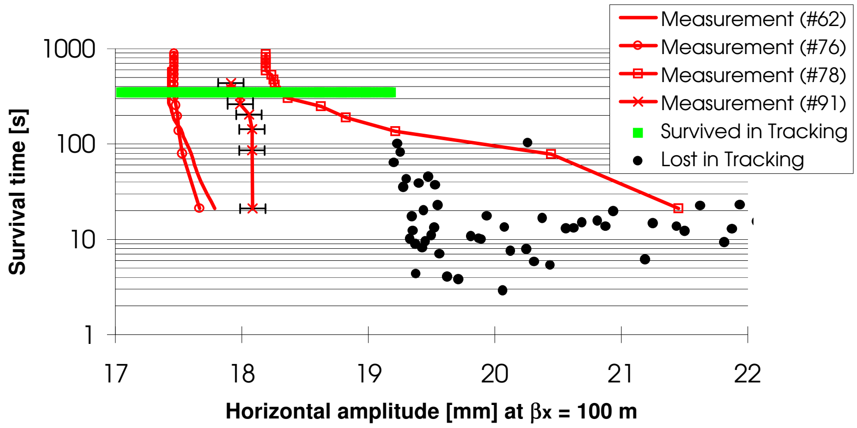

FIGURE 3: Dynamic aperture at WP1, tune modulation of 9Hz and $\Delta Q_x = 1.87 \cdot 10^{-3}$.

2.3 Dynamic Aperture Computations

The model included all sextupoles, the horizontal and vertical closed orbit, and the tune ripple. Tunes, chromaticities and linear coupling are adjusted similar to what was measured in the SPS. As the beam is kicked horizontally the particles are tracked with large horizontal displacements. Moreover, a vertical displacement of roughly one σ of the vertical beam size has been considered.

In all tracked cases a wide amplitude range could be found (column three in Tab. 2) where chaotic (after 200,000 turns) and regular regions alternate. Thus, the onset of chaotic motion gives a much too pessimistic estimate for the dynamic

TABLE 2: Comparison of measured and computed horizontal dynamic aperture in the SPS experiment. All values are given for $\beta_x = 100$ m. For the onset of chaos there are two values: the larger one is the border above which no regular particles could be found, the lower (in brackets) is the lowest amplitude at which large scale chaotic motion sets in. The measured dynamic aperture and the loss border are both determined after 345 s.

case	measured dynamic aperture $a_{x,meas}$ [mm]	onset of chaos in tracking ($2 \cdot 10^5$ turns) $a_{x,chaotic}$ [mm]	loss border in tracking ($1.5 \cdot 10^7$ turns) $a_{x,loss}$ [mm]	relative difference between measurement and loss border $\left(\frac{a_{x,loss}}{a_{x,meas}} - 1\right)$ [%]
WP1, 9 Hz, $\Delta Q_x = 1.87 \cdot 10^{-3}$	17.4	(7.7) 14.3	19.2	10
WP2, 9 Hz, $\Delta Q_x = 0.55 \cdot 10^{-3}$	19.5	(7.4) 8.3	22.3	14
WP1, natural ripple only	20.0	(15.7) 23.1	24.4	22
WP2, natural ripple only	20.9	(9.8) 23.6	25.7	23

aperture. In the following, we rely on long–term tracking for an estimate of the dynamic aperture. The results are shown in column four in Tab. 2. In the simulation 15 million turns (345 s storage time) could be reached with reasonable computing effort.

2.4 Comparison

The last column in Tab. 2 shows the relative difference in percent between the computed and the measured dynamic aperture. In the cases with additional tune modulation the difference is about 10% but without additional modulation this number rises to more than 20%. Moreover in the tracking we find a broad region of apparently regular motion outside the experimental stability border for the cases without additional tune modulation. From this we have to conclude that a destabilizing effect is missing in the simulation. A rough estimate for the magnitude of this effect is given by the strength of the additional tune modulation because the experimental dynamic aperture without extra tune modulation agrees well with that of the tracking when this modulation is introduced (compare the last two entries in column two with the first two entries in column four of Tab. 2). The nature of this effect is still not yet understood, a discussion can be found in Fischer[4].

3 THE EXPERIMENT AT THE HERA PROTON RING

In the HERA proton ring nonlinearities are introduced through the field errors of the superconducting magnets. These errors are known in great detail. Each individual magnet was cold tested and the multipole errors were recorded at several excitation levels. In addition, at injection level the decay of the persistent currents was measured. Results of those measurements are available from publications (cf. Schmüser[5] and Brück[6]) and from a data basis.

The experiments were done under conditions similar to those at injection in normal operation (see Tab. 1). Two working points were tested, one with well separated tunes (31.285, 32.303) and one close to the main coupling resonance (31.287, 32.287) referred to as WP3 and WP4 respectively (see Fig. 4 (*a*)). At the second working point measurements were also made with an additional tune modulation of 50 Hz and $\Delta Q_x = 2 \cdot 10^{-3}$ and with a compensation of three major tune ripple lines (cf. Brüning[3,8]).

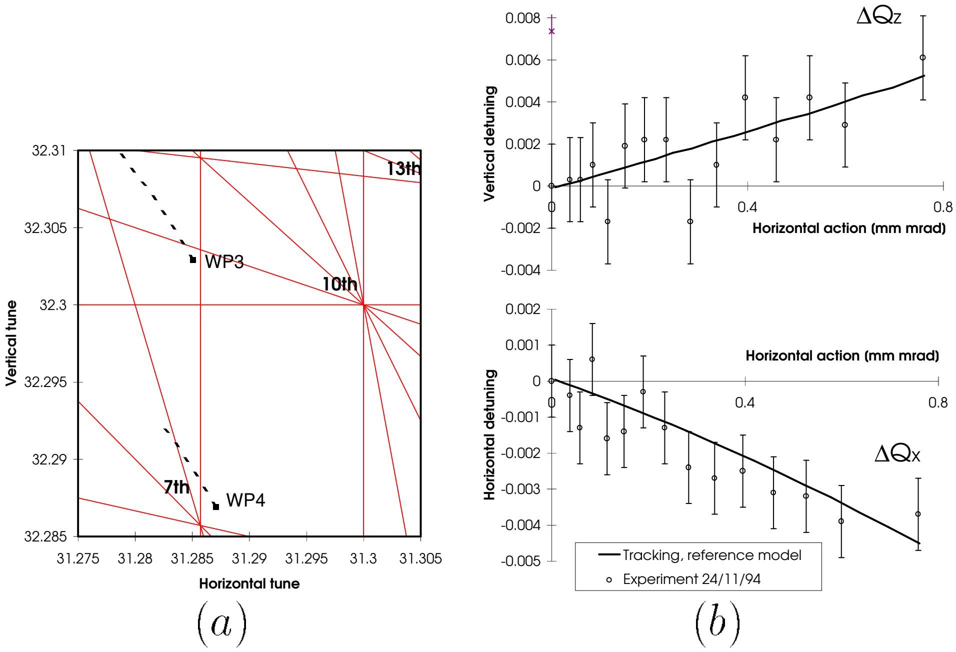

FIGURE 4: (*a*) The working points WP3 and WP4 in the tune diagram. Sum resonances up to order 13 are shown. The dotted lines show the detuning when the horizontal dynamic aperture is approached. (*b*) Detuning of the HERA proton ring at working point WP3 with the set–up given in Tab 1.

3.1 Detuning and Instrumentation

As in the SPS experiment, the amplitude dependent tunes were measured as a function of the horizontal action by kicking the beam with different kick strength (Fig. 4 (*b*)). In order to check the sensitivity of the detuning in the model with respect to variations in the input parameters different closed orbits, changes in the 10– and 12–pole correctors strength and changes in the sextupole configuration (variations in the strength of locally uncompensated sextupoles while keeping the

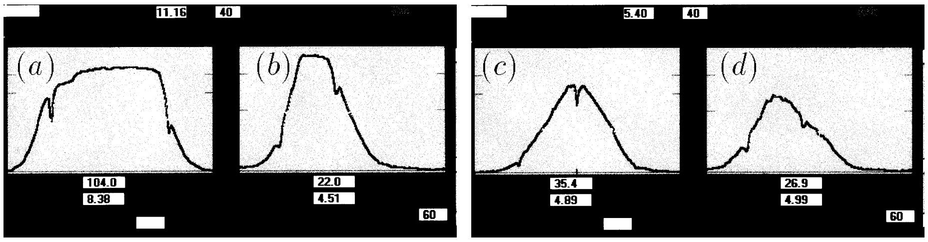

FIGURE 5: Beam profiles at two different times after a horizontal kick with a beam of 60 bunches. Part (*a*) and (*b*) show the horizontal and vertical beam profile respectively right after the kick, the horizontal profile (*c*) and the vertical profile (*d*) were taken 10 minutes later. The notches are markers to determine the width of the profile.

chromaticity compensated) were tested. Only the last variation showed a significant influence on the detuning. In the machine locally uncompensated sextupoles can be created since the decay rate of the persistent currents vary from magnet to magnet. In addition, only two reference magnets are used for the automatic chromaticity correction. They have to represent the average of the two different production lines. The reference model was chosen to properly return the measured detuning coefficients (Fig. 4 (*b*)).

For the dynamic aperture measurements the kicked beam was observed with a rest gas ionisation monitor. Its time constant of about 0.5 s, its resolution (0.1 mm) and its systematic error ($\approx 2\%$ of the measured width for the beam parameters under consideration) are sufficiently small to be neglected in the aperture measurements (see Schotmann[7]). Currents of about 1 μA ($1.5 \cdot 10^8$ protons) can be still observed.

3.2 Dynamic Aperture Measurements

Apart from measuring the dynamic aperture with rest gas beam profiles it was determined from beam loss measurements of a kicked beam of small transverse dimensions ("pencil" beam) assuming an scraped Gaussian particle distribution before the kick. The interesting outcome of this method is that one has to assume tails in the transverse particle distribution right after the kick to obtain consistent results for different kick strength. This method gives somewhat smaller results for the aperture than the profile measurements and is described in detail in Brüning[3]. In the following we will report on the measurements using rest gas beam profiles. All betatron amplitudes are normalized to 76 m, the maximum value in the arcs.

After kicking a shrinking of the base width of the horizontal beam profile went along with particle losses for about 10 min. Fig. 5 shows the horizontal and vertical beam profiles at two different times after the horizontal kick.

In Fig. 6 the results of such profile measurements are depicted. The right curve was measured at WP3 with 60 bunches, 0.2 mA per bunch and a residual beam current of 6–7 mA after the kick. It was confirmed by a second measurement which extended over only 120 seconds. The left curve was measured at WP4 (close to or within the coupling resonance) one day later and with only 10 bunches per

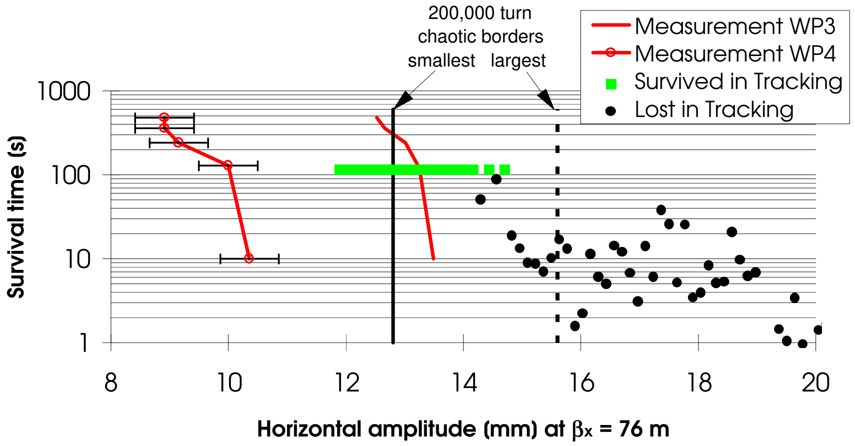

FIGURE 6: Dynamic aperture of the HERA proton ring at injection energy. The survival plot is shown for the reference model. In addition, the smallest and largest chaotic border of the tracking model, due to the variation of input parameters, is depicted as well.

beam. Measurements on the second day with additional tune modulation of 50 Hz and $\Delta Q_x = 2 \cdot 10^{-3}$ and with a compensation of the natural tune ripple lines at 100 Hz, 300 Hz and 600 Hz showed the same behavior at this working point within the measurement precision. The error bars are determined from the uncertainty of reading the beam profile base width in the rest gas monitor. In all cases investigated the measured horizontal edge of the beam distribution was significantly smaller than for the two cases measured one day before. The reason for this decrease in the dynamic aperture is not yet understood.

3.3 Dynamic Aperture Computations

All measured magnetic multipole errors including the time dependence of the largest persistent current components were included in the model (see Brüning[3], Fischer[4]). Closed orbit, linear coupling, tunes and chromaticity were adjusted to the experimental values.

The dynamic aperture is computed by two methods: firstly, the chaotic border is determined from the evolution of the distance of pairs of initially close–by particles (Lyapunov analysis), and secondly, by long–term tracking over 5 million turns (105 s storage time). To get an upper bound for the dynamic aperture, particles were launched in the horizontal plane only; vertical motion was introduced through coupling. The momentum amplitudes were $\Delta p/p \approx 1 \cdot 10^{-4}$ (0.66 σ of the longitudinal distribution). It was checked by tracking that particles with small momentum amplitude survive longer than particles with larger amplitudes.

A significant change in the dynamic aperture could only be observed after a variation of the strength of locally uncompensated sextupoles while keeping the chromaticity compensated at the same time. In Fig. 6 the survival plot of the reference model and the smallest and largest chaotic border (obtained under variation of the input parameters) is shown.

3.4 Comparison

The loss border in tracking (determined after 5 million turns or 105 seconds) was found to be less than 5% larger than the chaotic border. Therefore, it is justified to compare the measured dynamic aperture (determined after 500 s) with the chaotic border in the simulations.

In the experiments there is no adequate control of the vertical oscillation amplitudes due to uncorrected local coupling. The coupling is only corrected globally using two orthogonal skew quadrupoles. In the detuning measurements an amplitude ratio between vertical and horizontal betatron amplitudes of up to 39% could be observed. Therefore, the coupling should always be considered in the interpretation of the measured aperture data by using the total transverse aperture $a_{trans} = \sqrt{\beta(a_x^2 + a_z^2)}$.

Since the vertical amplitude of particles at the horizontal beam edge can not be determined in the experiments an interval for a_{trans} will be given, that is possible according to the coupling. For the measurements with separated tunes one obtains in this way a range for the total dynamic aperture after 500 s of $(12.6 - 13.5)$ mm (the upper bound is determined as 12.6 mm $\cdot \sqrt{1 + 0.39^2} = 13.5$ mm).

For the measurements on the coupling resonance an almost round beam was observed. Hence, the maximum total dynamic aperture should be $\sqrt{2}$ times the measured horizontal or vertical beam edge which gives an interval of $(8.8 - 12.4)$ mm.

In Tab. 3 the results are summarized. The larger number given in column four (relative difference between measurement and tracking) is a pessimistic estimate.

For the separated tunes the measured and computed dynamic aperture agree to within 20%. However, the residual coupling in the tracking was smaller than in the experiment and the amplitude ratio observed in the experiment was not reached for particles which were started with a vanishing vertical amplitude. Space charge effects were disregarded in the simulation. They would lead to a 10–20% change of the detuning coefficients (see Brüning[3]). Since the aperture is strongly dependent on the detuning this effect may explain part of the discrepancy.

On the coupling resonance the agreement between measured and computed dynamic aperture is worse than with separated tunes (Tab. 3). However, the experimental result that neither additional tune modulation with $\Delta Q_x = 0.002$ nor the compensation of the largest tune ripple frequencies changed the measured dynamic aperture at this working point is not understood. Theoretical estimates and the SPS experiments showed a clear dependence of the dynamic aperture on such a large tune ripple. Furthermore, the tune ripple compensation has been successfully applied under collision condition with beam–beam interaction to reduce the particle loss(see Brüning[8]).

4 CONCLUSIONS

For the SPS the measured and computed dynamic aperture agree within 10% when a tune ripple about 10 times stronger than the natural one was applied. This agree-

TABLE 3: Comparison of measured and computed dynamic aperture of the HERA proton ring at 40 GeV. All amplitude values are given for $\beta = 76$ m. The range of aperture for the measured values is determined by assuming a minimal or maximal vertical amplitude possible for the obtained horizontal beam edge using the measured coupling. The range in the computed aperture is obtained by varying input parameters.

case (Q_x, Q_z)		amplitude ratio a_z/a_x	transverse dynamic aperture $a_{trans} = \sqrt{\beta(a_x^2 + a_z^2)}$ [mm]	relative difference between measurement and tracking $\left(\frac{a_{trans,track}}{a_{trans,meas}} - 1\right)$ [%]
(31.285, 32.303)	measured	$\lesssim 0.39$	12.6–13.3	3–23
	tracking	≈ 0	12.8–15.6	
(31.287, 32.287)	measured	≈ 1	8.8–12.4	23–75
	tracking	≈ 0.8	15.4	

ment deteriorates for a smaller tune modulation depth and the relative difference reaches about 20% when only the natural tune ripple is considered. A 20% agreement between measurement and simulation could also be achieved for the HERA proton ring for the largest measured dynamic aperture.

ACKNOWLEDGEMENTS

The authors are thankful to all colleagues, engineers, technicians and operators, which were involved in the preparation and realization of the experiments, for discussions and help.

REFERENCES

1. F. Schmidt *SIXTRACK Version 1.2* (CERN SL/94–56 (AP) 1994, in WWW under: http://hpariel.cern.ch/frs/Documentation/doc.html)
2. W. Fischer, M. Giovannozzi and F. Schmidt *The Dynamic Aperture Experiment at the CERN SPS* (CERN SL/95–96 (AP) 1995, submitted to Physical Review E)
3. O. Brüning et al. *A Comparison of Measured and Calculated Dynamic Aperture of the HERA Proton Ring at Injection Energy* (DESY HERA 95–05 and CERN SL/95–69 (AP) 1995)
4. W. Fischer *An Experimental Study On the the Long–term Stability of Particle Motion in Hadron Storage Rings* (PhD thesis, Hamburg University, DESY 95–235, 1995)
5. P. Schmüser *Field Quality Issues in Superconducting Magnets* (proceedings of the IEEE Conference on Particle Accelerator Physics in San Francisco 1991)
6. H. Brück et al. *Time Dependence of Persistent Current Effects in the Superconducting HERA Magnets* (DESY–HERA 90–01 1990)
7. T. Schotmann *Das Auflösungsvermögen der Restgasionisations–Strahlprofilmonitore für Protonenstrahlen in PETRA und HERA* (in German, DESY HERA 93–09, 1993)
8. O. Brüning and F. Willeke *Reducing the Particle Loss in Hadron Storage Rings by Generating an Additional Harmonic Tune Modulation* (proceedings of the IEEE Conference on Particle Accelerator Physics in Dallas 1995)